Relationship between single quantum-dot intermittency and fluorescence intensity decays from collections of dots

Inhee Chung and Moungi G. Bawendi

Department of Chemistry and Center for Materials Science, Massachusetts Institute of Technology, 77 Massachusetts Avenue, Cambridge, Massachusetts 02139, USA

We show that the slow dynamics of the fluorescence from a collection of colloidal quantum dots and the intermittency observed in single quantum dots are intimately related. This system illustrates the importance of uncovering dynamical behavior at the microscopic level for a proper understanding of ensemble phenomenology. We propose a model that introduces lower and upper bounds to the on- and off-time power-law distributions in single-nanocrystal quantum-dot (QD) fluorescence intermittency statistics. We use Monte Carlo simulations and analytical forms to quantitatively connect this single QD model to the fluorescence intensity decay to a steady state that is observed in collections of QD's. Inversely, we also show that experiments on collections of QD's can be used to directly obtain upper bounds to the single-QD fluorescence intermittency power-law statistics.

PACS number(s): 78.67.Hc, 78.67.Bf

Although advances in single-fluorophore spectroscopy[1–3] have catalyzed detailed studies of individual fluorophores, connecting the dynamical behavior of a collection of fluorophores to that of the individual fluorophores is not always apparent, yet the phenomenology observed at the ensemble level must reflect the underlying microscopic dynamics. For example, while fluorescence spectroscopy on single-colloidal semiconductor quantum dots (QD's) has uncovered interesting fluorescence intermittency[4,5] phenomena, the implications of this intermittency to observations at the ensemble level have not been obvious. Inversely, it has not been clear how observations at the ensemble level can contribute to our understanding of the dynamics at the single-QD level. Yet understanding this connection is likely to be very important if we are to begin to understand the microscopic reasons for intermittency and also because the performance of QD's in applications ranging from biological imaging[6,7] to optoelectronic devices[8,9] increasingly appears to be strongly affected by the intermittency. The working hypothesis for colloidal QD's is that the intermittency results as the QD switches between an emissive, neutral state (bright or "on") and a nonemissive, ionized, charged state (dark or "off").[4,10–12] Probability distributions for the lengths of on (off) times have been experimentally shown to follow power-law statistics.[4,5] Interestingly, the characteristic powers for the on- (off-) time distributions have been observed to be similar and insensitive to environmental changes.[5] The measured powers, in the absence of bounds to the time range of the distribution, place the blinking effect in Lévy's statistical regime, where the mean and variance of the distribution diverge.[13] Upper bounds to the power law[5] have been observed only for the on times, but they must also exist for the off times. Otherwise, the emission intensities of all collections of QD's would eventually go to zero, which they do not. Emission intensities do exhibit a decay in time, but to a steady state. This decay has often been attributed to a permanent photochemical process. Although such processes can and do occur, decays observed under our experimental con-

ditions are reversible. We show here that intermittency by itself predicts and explains both the rate of decay and the ultimate steady-state level. Indeed, the behavior of a collection of QD's must reflect the underlying statistics of single QD's. This can be experimentally realized by exciting a collection of QD's that are immobile under the same conditions of high excitation power used to observe single QD's. Brokmann *et al.*[14] have explained the experimental intensity decay of a collection of QD's from single-QD statistics by taking a slightly higher on-time power than off-time power, which results in nonergodic behavior as expected from unbounded Lévy statistics, but this predicts a decay to zero intensity. Here we show that the experimentally observed intensity decay to a steady state in the fluorescence of a collection of immobile QD's implies that both on and off times must have upper bounds in their distributions and reflects underlying ergodic behavior. In this work, we propose a phenomenological model that introduces lower and upper bounds to the on- (off-) time power-law distributions of single-QD fluorescence intermittency. We use Monte Carlo simulations and analytical studies to show that this model is consistent with the intensity decay to a steady state observed in collections of immobile QD's. Finally, we show that parameters of the underlying single-QD phenomenological model that would be inaccessible from single-QD experiments can be obtained from experiments on collections of QD's.

Experimental time traces of fluorescence intermittency, by necessity, use a time binning process. We begin by showing that the measured statistics of on (off) times are not fundamentally affected by the choice of bin size, as long as it is sufficiently smaller than any experimentally observed long-time bound. For the purposes of this discussion, we define an "intrinsic" intensity time trace as a time series of emitted photons prior to an experimental binning process. We use the simplifying assumption that (1) an off state is a charged state that is "dark," (2) a photon is emitted after each absorption process during an on state, and (3) the shortest time scale is
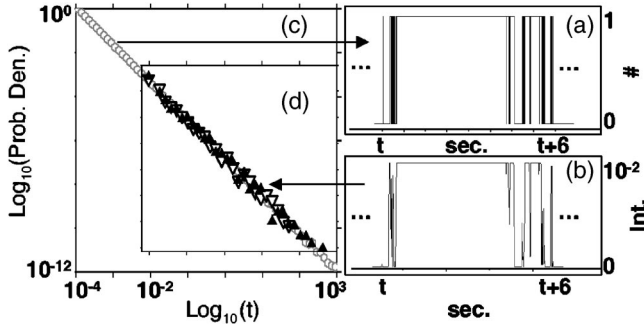
FIG. 1. (a) Small portion of a simulated intrinsic time trace, constructed from the on- (off-) time power-law probability distributions of Eq. (1) as described in the text. (b) Portion of the time trace [same portion as in (a)] after rebinning with a bin size of 10^{-2} sec. (c) Probability density distributions for on and off times (overlapping open circles) from Eq. (1), used to generate the time traces in (a) and (b), with powers $-\mu_{on(off)}-1=-1.5$. (d) Probability density distributions for on (open triangles) and off (solid triangles) times, extracted from the rebinned trace, a small portion of which is shown in (b). The intensity threshold defining on times is set to zero.

then determined by the excitation flux. This shortest time scale becomes an operational measure of the lower bound to the distributions of on (off) times. This intrinsic time trace effectively has a bin size determined by the inverse value of the excitation flux, returning a value of "1" if the QD is neutral (i.e., fluoresces when interrogated) or "0" if it is dark. As defined, the intrinsic time trace is then perfectly binary, as shown in the trace of Fig. 1(a), obtained using a Monte Carlo simulation described below. Rebinning this time trace, as is effectively done experimentally, diminishes its binary characteristic as shown in Fig. 1(b). The new bin size then sets a new operational lower bound for the on- (off-) time distributions. On (off) times in the rebinned time trace are defined relative to an arbitrary intensity threshold. To explore the effects of rebinning and the choice of intensity threshold, we simulate intrinsic time traces assuming bounded power-law statistics for the distributions of on (off) times:

$$p_{on(off)}(t)dt = 0 \ (t < t_{on(off)}^{min}), \ p_{on(off)}(t)dt = 0 \ (t_{on(off)}^{max} < t),$$

$$p_{on(off)}(t)dt = C_{on(off)}t^{-\mu_{on(off)}-1}dt \ (t_{on(off)}^{min} < t < t_{on(off)}^{max}),$$

$$(1)$$

where $p_{on(off)}(t)dt$ are on- (off-) time probability density functions, $C_{on(off)}$ are normalization factors, and $[t_{on(off)}^{min}, t_{on(off)}^{max}]$ defines the time interval for which power-law statistics hold. Consistent with experimental observations, we chose $\mu_{on(off)}=0.5$ (Refs. 10 and 11) and $t_{on(off)}^{min}=10^{-4}$ sec (the initial bin size). We arbitrarily set $t_{on(off)}^{max}=10^3$ sec, an order of magnitude larger than the longest experimentally observed off time (itself restricted by the length of an experimental time trace). Simulations were typically run to generate time traces spanning 3×10^5 sec. Figure 1(a) shows a small (6 sec) snapshot of an intrinsic time trace generated by this simulation. Figure 1(b) shows the same snapshot after rebinning, with a bin size of 10^{-2} sec. Figure
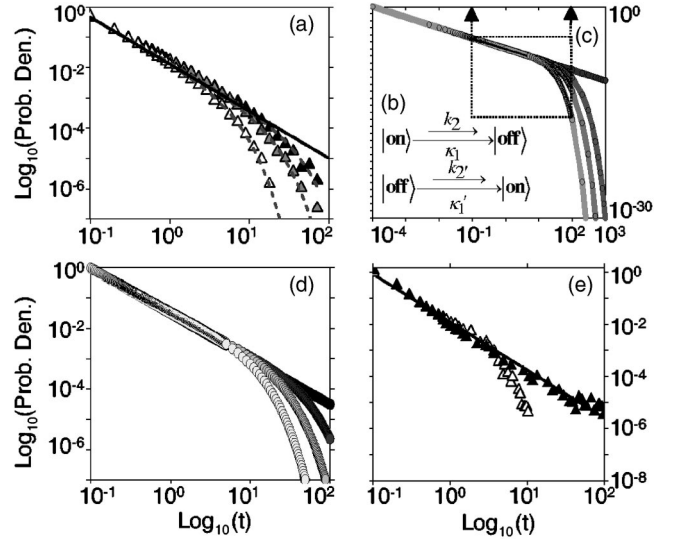

FIG. 2. (a) Experimental probability density distributions of the on times (triangles) for 1.5-nm-radius (black) and 2.5-nm-radius (gray) (CdSe)ZnS (core) shell QD's, and 2.5-nm-radius CdSe QD's (white). Their off-time distributions are indistinguishable on this graph and plotted as a solid line. The dashed lines are fits using Eq. (2), giving $\tau_{on}=16.4, 7.8,$ and 2.7 sec, respectively. The bin size in these experiments was 10^{-1} sec. (b) Phenomenological half-reaction schemes for the two switching channels between on and off states, as described in the text. (c) Calculated probability density distributions using Eq. (2) with $\tau_{on}=20, 5,$ and 2 sec, $\tau_{off}=10^3$ sec, and $t_{on(off)}^{min}=10^{-4}$ sec. The dotted box indicates the experimental time range of $[10^{-1}, 10^2]$ sec. (d) Calculated probability density distributions in the dotted box of (c), renormalized for comparison with the experimental data in (a). (e) Probability density distributions for on times (open triangles) and off times (black triangles) obtained from a simulated time trace using Monte Carlo methods from Eq. (2), using $\tau_{on}=2$ and $\tau_{off}10^3$ sec, and rebinned (bin size=10^{-1} sec).

1(c) (open circles) shows the probability density distributions of on (off) times used to generate the intrinsic trace. The probability density distributions of on and off times extracted after rebinning are shown as open and solid triangles in Fig. 1(d), using an intensity threshold set to 0 to define on and off events. Changing the intensity thresholds did not change the measured power-law statistics. Simulations were also performed to test different intrinsic power-law statistics with $0 < \mu_{on(off)} < 1$, defined in the same range $[10^{-4}, 10^3]$ (sec). We found in every case that the intrinsic power-law statistics was preserved through the rebinning process.

Experimental on-time distributions are observed to deviate from a pure power law at longer times. This deviation is observed as a decay, or roll-off, away from the power law, or as an abrupt cutoff of the power-law distribution if the time trace is not long enough to statistically acquire enough of the long on-time events in this decay. Figure 2(a) shows experimental probability density distributions of on times (triangles) and off times (straight line), collected from various QD's (Ref. 5) at room temperature. At low temperature (10 K) and low laser excitation flux,[5] the on-time power law was observed to extend as far as the off-time power law

within the experimental window available. The deviation from the power law implies that the on-time power-law statistics occurs in parallel with additional channels for charging the QD's that effectively act as upper bounds to the power law. These additional channels are affected by the surface environment of the QD's, the temperature, and the excitation intensity.[5] Protecting the surface of the QD's increases the probability of observing longer on times, delaying the start of deviation from power-law statistics. Upper bounds or deviations from power-law statistics for the off times have not been observed experimentally. That is because these bounds are apparently significantly longer than those for the on times, as is seen below in our analysis of decays of collections of QD's.

We now construct a phenomenological model that incorporates the experimental observations as follows. We construct waiting time distributions with the half-reaction schemes as seen in Fig. 2(b), where each half-reaction consists of two parallel switching channels. One channel gives rise to a power-law distribution [resulting, for example, from an appropriate distribution of rate constants $k_{1(1')}$ (Ref. 11)], and the other, responsible for the upper bounds, is exponential with rate constants $k_{2(2')}$. The waiting time distributions $p_{nf(fn)}(t)dt$, are the probability densities for observing a switch from an on state to an off state (nf) or vice versa (fn) after residing in an on or off state for a time t. Consequently $p_{nf(fn)}(t) = dP_{on(off)}(t)/dt$, where $1 - P_{on(off)}(t)$ are the cumulative distribution functions for on (off) times [i.e., the probability that a QD still remains "on" ("off") a time t after the last switching event] and

$$1 - P_{on(off)} = C_{on(off)} t^{-\mu_{on(off)}} \exp(-t/\tau_{on(off)})$$
$$\times (t_{on(off)}^{\min} < t), \quad P_{on(off)} = 0 \quad (t < t_{on(off)}^{\min}) \quad (2)$$

with $\mu_{on(off)} = 0.5$ to match experiments and with $t_{on(off)}^{min}$ as operationally defined lower bounds as described previously. The exact values of $t_{on(off)}^{min}$ do not affect our results, as long as they are significantly smaller than both the length of a complete time trace and τ_{on}. The exponential term in the probability distribution effectively acts as an upper bound to the power law. The presence of a lower bound and the exponential cutoff enables calculation of normalization factors $C_{on(off)}$. We use this model to fit the experimental data of Fig. 2(a) (dashed lines), extracting τ_{on} values of 16.4, 7.8, and 2.7 sec for 1.5-nm-radius (CdSe)ZnS [(core) shell] QD's, 2.5-nm-radius (CdSe) ZnS QD's, and 2.5-nm-radius CdSe QD's, respectively. Figure 2(c) shows calculated probability density functions $p_{nf(fn)}(t)$ based on Eq. (2) with on- (off-) time probability distributions created with $\tau_{on} = 20$, 5, and 2 sec, $\tau_{off} = 10^3$ sec [chosen to be larger than the experimentally observed longest off-time in Fig. 2(a)], and $t_{on(off)}^{min} = 10^{-4}$ sec. Restricting the data between 10^{-1} sec and 10^2 sec and rescaling shows that the calculated probability densities of Fig. 2(d) compare well with their corresponding experimental counterparts in Fig. 2(a). These statistics are also robust to rebinning. An intrinsic time trace constructed using Monte Carlo methods from Eq. (2) using $\tau_{on} = 2$ sec and $\tau_{off} = 10^3$ sec was rebinned using a bin size of 10^{-1} sec. The

on- (off-) time statistics of the rebinned time trace were then obtained and plotted in Fig. 2(e), which closely matches the experimental white triangle plot in Fig. 2(a).

With a phenomenological model for single-QD statistics put forth, we now turn to the behavior of the fluorescence intensity from collections of immobile and dilute (noninteracting) QD's. Figure 3(a) shows intensity time traces from two different samples of (CdSe)ZnS QD's, normalized to the initial intensity. The samples are in the dark until $t = 0$, when they are then illuminated with the laser. Both samples show fluorescence intensity decays, reaching steady-state values at ~ 680 and 3900 sec, respectively. The existence of a steady state implies that the power-law distribution of off times must also have an upper bound and that the system is ergodic. Otherwise the intensity evolutions would statistically "age," decaying to zero, with all the QD's displaying nonergodic behavior by eventually residing in nearly infinitely long off states. The intensity time trace of a collection of immobile, dilute QD's can be identically mapped onto the probability of finding a single QD in an on state. We can therefore analyze this ensemble experiment within the context of our phenomenological model for the statistics of single QD's. We will proceed two ways. We will derive analytical expressions for the probability of finding a QD to be "on," and we will also simulate time traces for many individual QD's using Monte Carlo methods, and add these traces together.

Analytical expressions for the probability of a QD being "on" can be derived from the waiting time distributions $p_{nf(fn)}(t)$. This probability, defined as $f_{on}(t)$, can be expressed in its Laplace transform[13]

$$f_{on}(s) = \alpha f_{nn}(s) + (1-\alpha)f_{fn}(s) = \frac{\alpha + (1-\alpha)p_{fn}(s)}{1 - p_{fn}(s)p_{nf}(s)} \frac{1 - p_{nf}(s)}{s},$$
$$(3)$$

with

$$f_{nn}(s) = \frac{1}{1 - p_{fn}(s) \cdot p_{nf}(s)} \frac{1 - p_{nf}(s)}{s},$$

$$f_{fn}(s) = \frac{p_{fn}(s)}{1 - p_{fn}(s)p_{nf}(s)} \frac{1 - p_{nf}(s)}{s}, \quad (4)$$

where $f_{nn}(s)$ is the probability that a QD is "on" at time t, given that it is "on" at $t = 0$, $f_{fn}(t)$ is the probability that a QD is "on" at time t, given that it is "off" at $t = 0$, and α is the proportion of QD's that are "on" at time $t = 0$. To solve for $f_{on}(s)$, we divide the time into three regions as shown in Fig. 3(b): $t_{on(off)}^{\min} \ll t < \tau_{on}$, $\tau_{on} \ll t < \tau_{off}$, and $\tau_{off} \ll t$. The behavior of $f_{on}(t)$ in the initial time range $0 \leq t \sim t_{on(off)}^{\min}$, which is thus far experimentally inaccessible, will be described elsewhere. We obtain the following results, as explained below, where $\langle t_{on(off)} \rangle$ is the expectation value for on (off) times:

$$f_{on}(t) \cong 0.5, \quad t_{on(off)}^{\min} \ll t < \tau_{on},$$

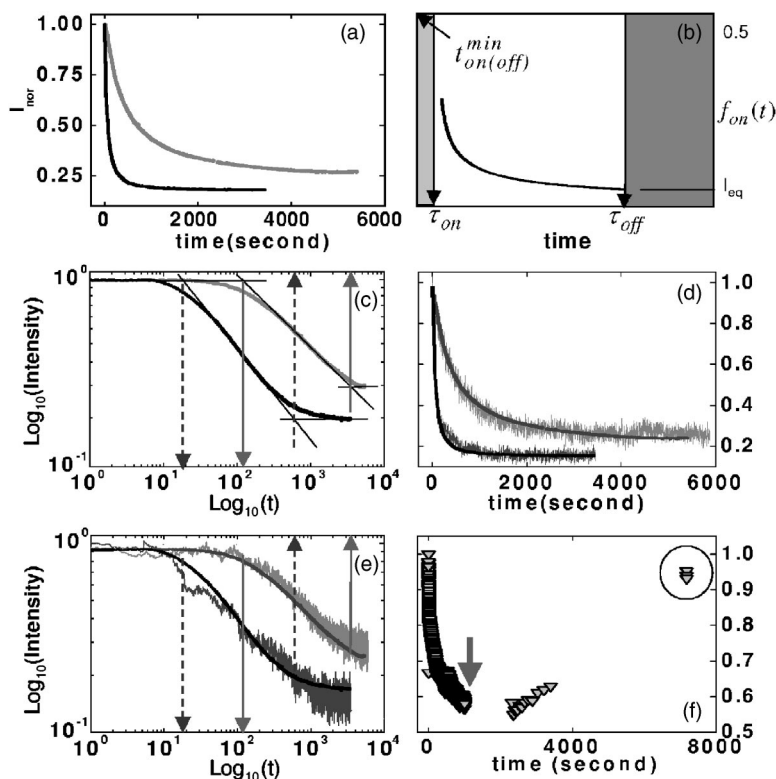$$f_{on}(t) \propto t^{-(1-\mu_{off})}, \quad \tau_{on} \ll t < \tau_{off},$$

FIG. 3. (a) Normalized fluorescence intensity time traces from two collections of different (CdSe)ZnS (core) shell QD's with core radii of 2.5 nm (black and gray). (b) Plot of the analytical form for $f_{on}(t)$ [Eq. (3)]. (c) Log-log plots of the experimental intensity time traces in (a). The beginning and end points of the power-law decays for the two plots are indicated by arrows pointing up for the beginning points and pointing down for the end points, respectively. These points are obtained as the intersections of the two slopes. These points experimentally determine τ_{on} and τ_{off}. (d) Intensity time traces obtained from adding 5000 different time traces generated using Monte Carlo simulations. The smooth solid lines are the experimental data in (a) for comparison. (e) Log-log plots of the simulated intensity time traces in (d) with plots in (c) overlayed. (f) Observed fluorescence intensity recovery after an initial decay, as described in the text, obtained from a collection of 2.4-nm radius (CdSe)ZnS (core) shell QD's. The arrow indicates the time when continuous excitation was stopped.

$$f_{on}(t) = \frac{\langle t_{on} \rangle}{\langle t_{on} \rangle + \langle t_{off} \rangle}, \quad t \gg \tau_{off}. \quad (5)$$

When $t_{on(off)}^{min} \ll t < \tau_{on}$, $f_{on}(t)$ is at a transient steady state with $f_{on}(t) \cong 0.5$ (Ref. 15) that results from $t_{on}^{min} = t_{off}^{min}$. When $\tau_{on} \ll t < \tau_{off}$, an average value for on times can be calculated, so that a small-s expansion from Eq. (3) gives $p_{nf}(s) \sim 1 - s \langle t_{on} \rangle$, while $p_{fn}(t)$ is still a power law. Since the on-time distribution converges while the off-time distribution is still a power law in this region, the probability $f_{on}(t)$ decays like a power law with the power given as $1 - \mu_{off}$. Finally, when $t_{off}^{max} \ll t$, average values can be obtained for both on and off times. Then $p_{nf(fn)}(s) \sim 1 - s \langle t_{on(off)} \rangle$ and small-s expansions yield a steady state which is the ratio of the average on time to the sum of average on and off times.

These analytical forms for $f_{on}(t)$ are especially interesting because they directly link the intensity time trace of a collection of QD's to the statistical parameters that describe the phenomenology of single-QD on- (off-) time distributions. In other words, experiments on collections of QD's can be used to extract the phenomenological parameters of single-QD statistical models. This is particularly powerful because experiments on collections of QD's can access regimes (such

as long effective time traces or low laser flux intensities) that are inaccessible with single-QD experiments. The main result is that $f_{on}(t)$ should behave as a power law for $\tau_{on} \ll t < \tau_{off}$ and should level out to a constant defined by τ_{on} and τ_{off} for $t \gg \tau_{off}$. This is confirmed experimentally by taking the experimental decays of Fig. 3(a) and replotting them on a log-log scale in Fig. 3(c). After an initial flat region, the two curves show a power-law decay with a power of approximately -0.5 (as expected from single-QD statistics) starting at $t \sim 14$ and 110 sec after $t = 0$ sec. After passing these transition points at $t \sim 14$ and 110 sec, the two plots begin to deviate from a power law at $t \sim 680$ and 3900 sec and enter steady-state regions, as predicted by Eq. (3). The beginning (14 and 110 sec) and end (680 and 3900 sec) of the power-law regime thus correspond to experimental values for the average single QD phenomenological constants τ_{on} and τ_{off}. This represents the first experimental observation of an effective upper bound for the length of off times. As an illustration of the significance of this result, we estimate that it would require a single-QD intensity time trace that is $\sim 10^6$ sec (2 weeks) long to extract such a value of $\tau_{off} \sim 3900$ sec. The steady-state saturation intensities for $t \gg \tau_{off}$ are obtained experimentally as $I_{sat} = 0.10$ and 0.13 for the two curves, which compares well with the prediction of Eq. (3), which, using the experimentally determined values

for τ_{on} and τ_{off}, predicts $I_{sat}=0.12$ and 0.14, respectively.[16] We have observed and measured effective upper bounds for on and off times and steady-state saturation intensities for many other QD samples, indicating that our model appears to be quite general for colloidal QD's.

To further complete the picture, we simulate the intensity time trace of a collection of QD's by summing the time traces of many individual QD's. We use the values of τ_{on} and τ_{off} experimentally obtained above to generate intensity time traces for 5000 QD's by Monte Carlo methods, using a bin size of 10^{-1} sec. The summation of these traces is shown in Figs. 3(d) and 3(e). The simulated time traces overlap well with the experimental traces. The intensity fluctuations observed in the simulated traces are consequences of the finite number of QD's in the collection, with each QD blinking.

If the experimental intensity decays of collections of QD's in Fig. 3 are the result of underlying single-QD statistics, then this intensity decay should be reversible. This is illustrated in Fig. 3(f). The initial intensity decay in the presence of continuous excitation is first observed. The excitation light was removed at $t=1400$ sec (marked by an arrow), and the fluorescence intensity was then sampled with short excitation events. The intensity as shown inside a circle is observed to have almost completely recovered after 6400 sec. This recovery also indicates that the switch from an off to an on state need not be light induced.

In conclusion, we have shown that bounds to the power-law probability distributions for on and off times in QD blinking statistics are critical in understanding fluorescence intermittency in these fluorophores. These bounds allow us to quantitatively correlate the properties of single QD's to the observation of intensity decays in collections of QD's, under conditions where permanent photochemical darkening processes appears to be insignificant. Most importantly, with these bounds, a collection of QD's behaves theoretically and experimentally as an ergodic system. The upper bounds for off times, inaccessible with single-QD experiments, have been consistently observed in fluorescence time traces from many other collections of QD's. The presence of a steady state at longer times in the fluorescence traces is fundamentally different from the nonergodicity claimed in previous works.[14] We have shown that experiments on collections of QD's can now also be used to extract parameters of single-QD statistics that could not have been obtained otherwise. These new parameters are likely to have a microscopic origin. A systematic exploration of how these parameters vary as a function of local QD environment may be the key to understanding intermittency at the microscopic level. Finally, this study provides an understanding of the photodarkening process of collections of chromophores, a process that is often unclear in its origins, based on the dynamics of single chromophores.

---

[1] W. E. Moerner and L. Kador, Phys. Rev. Lett. **62**, 2535 (1989).

[2] M. Orrit and J. Bernard, Phys. Rev. Lett. **65**, 2716 (1990).

[3] E. Betzig and R. J. Chichester, Science **262**, 1422 (1993).

[4] M. Kuno, D. P. Fromm, H. F. Hamann, A. Gallagher, and D. J. Nesbitt, J. Chem. Phys. **112**, 3117 (2000); **115**, 1028 (2001).

[5] K. T. Shimizu, R. G. Neuhauser, C. A. Leatherdale, S. A. Empedocles, W. K. Woo, and M. G. Bawendi, Phys. Rev. B **63**, 205316 (2001).

[6] M. Dahan, S. Levi, C. Luccardini, P. Rostaing, B. Riveau, and A. Triller, Science **302**, 442 (2003).

[7] D. S. Lidke, P. Nagy, R. Heintzmann, D. J. Arndt-Jovin, J. N. Post, H. E. Grecco, E. A. Jares-Erijman, and T. M. Jovin, Nature (London) **22**, 198 (2004).

[8] N. Tessler, V. Medvedev, M. Kazes, S. H. Kan, and U. Banin, Science **295**, 1506 (2002).

[9] W. K. Woo, K. T. Shimizu, M. V. Jarosz, R. G. Neuhauser, C. A. Leatherdale, M. A. Rubner, and M. G. Bawendi, Adv. Mater. (Weinheim, Ger.) **14**, 1068 (2002).

[10] Al. L. Efros and M. Rosen, Phys. Rev. Lett. **78**, 1110 (1997).

[11] M. Kuno, D. P. Fromm, S. T. Johnson, A. Gallagher, and D. J. Nesbitt, Phys. Rev. B **67**, 125304 (2003).

[12] Y. Jung, E. Barkai, and R. J. Silbey, Chem. Phys. **284**, 181 (2002).

[13] F. Bardou, J. P. Bouchaud, A. Aspect, and C. Cohen-Tannoudji, *Lévy Statistics and Laser Cooling* (Cambridge University Press, Cambridge, England, 2001).

[14] X. Brokmann, J.-P. Hermier, G. Messin, P. Desbiolles, J.-P. Bouchaud, and M. Dahan, Phys. Rev. Lett. **90**, 120601 (2003).

[15] Starting from $f_{on}(0)=\alpha$, $f_{on}(t)$ evolves to a transient steady state that lasts while $t_{on(off)}^{min} \ll t < \tau_{on}$ with a value determined only by t_{on}^{min} and t_{off}^{min}. This transient steady state results from the high probability of short on and off times. This fast switching between on and off times establishes a steady state with an intensity value determined by the ratio $t_{on}^{min}/t_{off}^{min}$ and by the exponent for the power laws for the on and off times. Since we (1) arbitrarily set $t_{on}^{min}=t_{off}^{min}$ in our paper and (2) set the on and off times to have the same power-law statistics, $f_{on}(t_{on(off)}^{min} \ll t < \tau_{on})=0.5$, $t_{on}^{min} \neq t_{off}^{min}$ would result in $f_{on}(t_{on(off)}^{min} \ll t < \tau_{on}) \neq 0.5$.

[16] Note that Eq. (3) has $I(t=0)=0.5$, while we normalized Fig. 3 to have $I(t=0)=1.0$. This is taken into account in our comparison.